

Investigations on the Geometric Accuracy of the NavVis VLX 2 and VLX 3 Systems for the Use in Indoor Applications

Thomas P. Kersten¹, Malte Marsmann¹

¹ HafenCity University Hamburg, Photogrammetry & Laser Scanning Lab, Henning-Voscherau-Platz 1, 20457 Hamburg, Germany
[Thomas.Kersten, Malte.Marsmann]@hcu-hamburg.de

Keywords: 3D, accuracy, mobile systems, quality, simulation, test field.

Abstract:

Mobile mapping technology from NavVis GmbH enables buildings and interiors to be captured quickly and accurately, creating digital twins. At HafenCity University (HCU) Hamburg, the NavVis VLX 2 and VLX 3 were used to test an interior recording system and compare it with reference data from the Z+F IMAGER 5016 terrestrial laser scanner. Geometric accuracy was analysed using two 3D test fields in the HCU Hamburg geodetic laboratory. During the investigations, the spatial distances in the 3D test fields showed an average deviation of 6 mm and a maximum deviation of 18 mm without control points, and 4 mm with a maximum deviation of 14 mm with control points. Various error simulations were performed, introducing gross errors of up to 20 cm in individual control point coordinates, some of which could be detected. When the 3D point clouds were compared with the Z+F IMAGER 5016 static terrestrial laser scanner reference, slight shifts in the point cloud were observed depending on the distance to the control points. However, these shifts were within the manufacturer's accuracy specifications and ranged from a few millimetres. The laboratory tests proved that the NavVis VLX 2 and VLX 3 are very efficient, easy-to-use indoor recording systems.

1. Introduction

In recent years, the ongoing digitisation of buildings and infrastructure has significantly changed the field of geodesy. Building Information Modelling (BIM) and the development of digital twins, in particular, are becoming increasingly important for users and manufacturers alike. Against this backdrop, Munich-based NavVis GmbH presents NavVis VLX 2 (second generation) and VLX 3 (third generation): a technology solution that enables the efficient and precise capture of buildings and interiors. When combined with NavVis IVION software, the NavVis VLX systems offer high-quality, high-resolution, user-friendly recording capabilities, positioning them as the answer to the growing demand in the field of building information modelling and digital twins (NavVis, 2021).

The term 'digital twin' can be defined as a virtual representation of an object or process, which makes the underlying data intelligible and usable for various applications (Rosen et al., 2015; Digital Twin Consortium, 2022). Until the mid-2010s, mobile mapping was not widely used in everyday surveying (Fritsch, 2014). However, a paradigm shift is currently taking place. In a 2021 survey by NavVis, 72% of surveying service providers stated that laser scanning is most frequently used for 3D as-built documentation and building information modelling. 3D and BIM models come second, as documented by NavVis (2021). Additionally, Fritsch (2014) explains that the processing of large point clouds can be automated to circumvent demanding processing.

In the early days of mobile mapping, vehicles were used primarily for surveying purposes. Nowadays, however, portable systems such as those from NavVis also enable flexible and efficient data collection. According to Gebert (2023), there is already a trend towards fully automated data collection. Stachniss (2017) introduces and provides an overview of the mapping and simultaneous localisation of mobile sensor platforms. These developments demonstrate a paradigm shift in geodetic methods. They are shifting from traditional methods to innovative technologies. This paper presents an investigation into

the geometric accuracy of two NavVis systems in a laboratory setting. The aim is to demonstrate the potential of this new technology for geodetic applications.

2. Related Work

Studies on mobile mapping systems, and in particular the NavVis mobile mapping system, have already been summarised in previous literature. In their paper, Lehtola et al. (2017) analyse point clouds from eight systems: five commercial indoor mapping systems (Matterport, NavVis, Zebedee, Stencil and Leica Pegasus Backpack), and three research prototypes (Aalto VILMA, FGI Slammer and Würzburg Backpack). These point clouds were then compared to 3D point clouds collected using Leica ScanStation P40 and Faro Focus^{3D} terrestrial laser scanners at three different test sites with varying characteristics.

Haaranen (2022) analysed point clouds collected using three different laser scanners: the Navvis M6, the Navvis VLX, and the LiDAR sensor built into the iPhone 12 Pro Max. These were then compared to a reference point cloud that had been collected using a Leica RTC360 terrestrial laser scanner. On average, the deviation between points measured with the M6 and the reference point cloud was 8 mm. The average distance between the VLX and the reference point cloud was 13 mm. It is likely that the point cloud measured with the iPhone was deformed by the SLAM method.

As part of their research, Campi et al. (2022) analysed the NavVis VLX mobile recording system used to survey the crypt of the Cathedral of San Matteo in Salerno, Italy. Meanwhile, Schmidt et al. (2023) investigated how different recording methods influence the detection of hidden edges and corners in point clouds of interior spaces. These point clouds were acquired using a combination of the NavVis VLX mobile system, the Z+F IMAGER 5016 terrestrial laser scanner, and the Intel RealSense D455, employing the Visual Simultaneous Localisation and Mapping (VSLAM) method.

Askar et al. (2023) compared the performance of a modern mobile indoor mapping system (NavVis VLX) with that of a terrestrial laser scanner (Z+F IMAGER 5016) for documenting buildings in complex indoor environments. The study focused on the geometric accuracy of scanned interiors. The results show that the NavVis VLX mobile mapping system, with an accuracy better than 2.5 cm when comparing point clouds with the reference, and a low noise level, is promising for complex interior imaging.

Sekine et al. (2023) created a 3D environmental map of the National Institute of Technology campus in Tokyo using high-density, high-precision 3D point clouds from the NavVis VLX and LIO-SAM systems for a mobile robot. The target course was a full circuit of approximately 320 m, consisting only of outdoor scenery with stairs. The resulting map from the NavVis VLX enabled the robot to navigate the course autonomously with a high degree of accuracy and without difficulty.

Gharineiat et al. (2024) evaluated the accuracy of the NavVis VLX 2 and BLK2GO SLAM scanners for outdoor and indoor surveying tasks. For this study, reference data was generated using a Leica TS16 total station and a Z+F IMAGER 5016 static laser scanner. The following four comparisons were evaluated: cloud-to-cloud, cloud-to-mesh, mesh-to-mesh, and edge detection board assessment. The results confirmed that indoor SLAM scanner measurements were more accurate (5 mm) than outdoor measurements (between 10 mm and 60 mm). Additionally, the cloud-to-cloud comparison offered the greatest direct accuracy without manipulation.



Figure 1. The NavVis VLX 2 acquisition system strapped onto the surgeon's body (left) and during a control point measurement in the 3D test field (centre), and VLX 3 (right).

3. The NavVis Systems VLX 2 and VLX 3

The NavVis VLX 2 and VLX 3 are the second and third generations of the portable mobile mapping system developed by NavVis GmbH in 2021 (Figure 1). Both systems use a total of two laser scanners positioned perpendicular to each other, four cameras and an inertial measurement unit to record data. The VLX 2 uses two Puck Lite (VLP-16) laser scanners from Velodyne LiDAR, whereas the VLX 3 uses a different laser scanning system: the Hesai XT32M. The Velodyne Puck Lite is a compact LiDAR sensor designed for precise 3D environmental sensing in autonomous vehicles, robots, and other mobile platforms. The LiDAR sensor features a rugged yet lightweight design (Business Wire, 2020). The XT32M is Hesai's latest 32-channel mid-range second-generation LiDAR sensor specially designed for survey and mapping applications. It has more than

double the scan rate, a longer range and a larger field of view than the Puck Lite, as well as being lighter. The main technical specifications of the Velodyne Puck Lite VLP-16 and the Hesai XT32M are summarised in Table 1.

System	VLP-16	XT32M
Wavelength	903 nm	905 nm
Range precision	6 mm	5 mm
Max. range	100 m	300 m
Scan rate per scanner	300,000 pts/s	640,000 pts/s
Distance meas. method	ToF	ToF
Field of View (hz/v)	360° / 30°	360° / 40.3°
Weight	590 g	490 g

Table 1. Technical specifications of the Velodyne Puck Lite (VLP-16, NavVis, 2024a) and Hesai (XT32M, Hesai, 2025) laser scanner according to manufacturer.

The VectorNav VN-100 Inertial Measurement Unit (IMU), which consists of a 3-axis accelerometer, a gyroscope, a magnetometer, a barometric pressure sensor and a 32-bit processor, is integrated into both the NavVis VLX 2 and VLX 3. It is housed in a compact aluminium case (VectorNav Technologies, 2025). The VN-100 IMU's main specifications are summarised in Table 2.

Dimensions	36 × 33 × 9 mm
Weight	15 g
Data frequency	800 Hz
Rotational rate sensor - Heading	2 Grad
Rotational rate sensor - Roll/Pitch	0,5 Grad
Rotational rate sensor - Drift	5-7 Grad/h
Accelerometer - Drift	0,4 mm/s ²

Table 2. Technical specifications of the inertial measurement unit of the VectorNav VN-100.

In both systems, the four cameras of the NavVis VLX are located at the top of the unit and positioned at 90-degree angles to each other. This configuration enables 360-degree RGB images to be generated at 20 megapixels each using fisheye lenses with a focal length of 3.3 mm. HDR (high dynamic range) is used for image generation (f/2.4 aperture) to optimise exposure (NavVis, 2024a).

The entire sensor system of the VLX 2 and VLX 3 is housed in a frame made of carbon fibre and anodised, powder-coated aluminium. The system weighs 8.7 kg and measures 108 cm in height, 33 cm in width and 56 cm in length. Located in front of the user's chest is an AMOLED multi-touch display, which provides an initial overview of the measurement area. This display can be used for rough orientation in the room and provides an overview of the data already recorded during the measurement. The display can also be used to control and enter control points or separate points of interest (POIs). The system is powered by two battery packs, each consisting of two lithium-ion V-mount micro batteries. These can be changed during the measurement process without interrupting the recording. The operating time of the two batteries is specified as 1.5 hours. A 1 TB portable SSD is used for storage.

4. Geometric accuracy tests in the laboratory

The geometric accuracy analyses are divided into three sections. The first part analyses the accuracy of the NavVis system in the 3D test field, both with and without control points (Figure 3).

Various simulations were also used to analyse how the adjustment algorithm deals with possible errors in the control point coordinates. As a result, adjustments with and without control point coordinates were analysed, as well as a total of three further experiments or simulations involving faulty control point coordinates (Table 3).

E	PN	Type of manipulation	ΔX	ΔY	ΔZ
			[cm]		
1	P1	Input error	+10	0	0
2	P6	Polygon course error	+4	+10	-3
3	P1	Arbitrary error	+10	0	0
3	P6	Arbitrary error	0	0	-20
3	P10	Arbitrary errors	-2	+2	+2
3	P11	Arbitrary error	0	-4,4	0

E...Experiment, PN...Point Number

Table 3. Summary of three experiments with manipulated, erroneous control point coordinates.

The first experiment describes a transmission error in the control point file, whereby the X coordinate of control point 1 was falsified by 10 cm. Experiment 2 simulates an error in a previously measured polygon traverse that was used to determine the control point coordinates in the target system. The third and final experiment involves manipulating the adjustment with arbitrary and gross errors. To this end, several points were altered in various directions (Table 3).

The second part of the analysis involves comparing the analysed system with the Z+F IMAGER 5016 terrestrial laser scanner, which is used as a reference. This analysis is based on processing data recorded with the NavVis VLX 2 and VLX 3 systems, using error-free original control points. The generated 3D point clouds were then compared at various positions within the laboratory. Previous laboratory tests have demonstrated that the Z+F IMAGER 5016 terrestrial laser scanner achieves geometric accuracies of better than 1 mm in the horizontal section and up to 2 mm in the spatial section (Kersten & Lindstaedt, 2022).

In the third part of the investigation, the sphere spacing error was determined in a mobile 3D test field (Figure 5). This was achieved by using short, calibrated scales with a sphere at each end, with distances ranging from 1.7 m to 2.3 m, in accordance with VDI/VDE 2634 (2012).

5. Data acquisition

The investigations into geometric accuracy covered the northern part of the second and third floors of HafenCity University Hamburg (Figure 2). The geodesy laboratory and the two corridors with connecting staircases were surveyed. For illustration purposes only, the routes taken by the NavVis VLX 2 are marked in yellow in Figure 2. Particular attention was paid to the geodetic laboratory during data acquisition, as this served as the starting and finishing point for the measurements. This laboratory contains the control point targets that were used to georeference the scans in both the 3D (Figure 3) and mobile (Figure 8) test fields. The corridors on the second and third floors are narrow and elongated, with little texture and many glass façades.

Table 4 below summarises the results of the recordings made using the NavVis VLX 2/3 and the Z+F IMAGER 5016 terrestrial laser scanners. It gives an overview of the recording time, data processing, required instruments, file volume, and products generated by the two systems.



Figure 2. Overview of the recording test area in the HafenCity University Hamburg building (red frames represent reflections on window panes and yellow lines mark the route of VLX 2).

System	NavVis VLX 2 / 3	Z+F IMAGER 5016
Scan time	< 1h	ca. 5h
Data processing	automatic	automated
Equipment	VLX, control points (targets)	tripod, system, spheres (targets)
Data volume	1,87 / 4.4 GB	0,93 GB
Products	3D point cloud (RGB) & panoramic images	3D point cloud (RGB optional)

Table 4. Information on the recording of the test area.

6. Data evaluation and results

Chapter 6 is divided into four sections according to the different evaluation methods. The first three sections deal with spatial distances in two test fields, and the final section compares the point clouds with reference data. Data processing of the point clouds was carried out using the cloud-based software solution NavVis IVION.

6.1 Analysis the spatial distances in the 3D test field

Different control point configurations of the NavVis systems were analysed in the 3D test field of the Geodetic Laboratory (Figure 3). The reference measurement of the control points on which the analysis is based was carried out in 2019 with excellent accuracy using a Leica ATR 960 laser tracker. This test field is also used for regular terrestrial laser scanner studies (Kersten & Lindstaedt, 2022). The coordinates of the 20 targets (control points) were measured manually in CloudCompare.

Due to the lack of georeferencing, the adjustment without control points only allows the distances between the reference points to be considered. Figure 4 shows that the deviations of the 105 determined spatial distances of the VLX 2 point cloud are less than two centimetres. The largest deviation found was -18 mm, while the standard deviation of the distance differences was 5.9 mm, with only two values falling outside the 95% confidence interval.

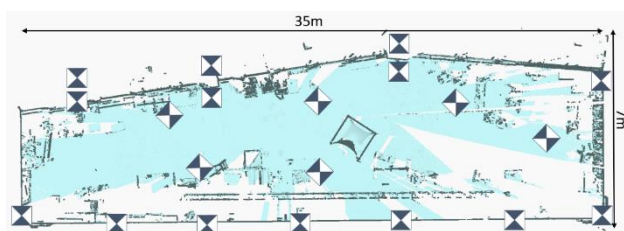


Figure 3. 3D test field in the geodetic laboratory at HafenCity University Hamburg with 20 reference points on the ceiling (rotated targets) and on the walls.

When adjusting with four control points, two of which were measured twice, the improvements in the coordinates of the control points were 1–2 mm, with maximum deviations in spatial distances of -15.1 mm and +6.0 mm for the VLX 2 and -11.7 mm and +7.2 mm for the. The span, defined as the absolute sum of the two maximum deviations, is 21.1 mm (VLX 2) and 18.9 mm (VLX 3). The mean deviation of -3.8 mm (VLX 2) and -1.0 mm (VLX 3) in Table 5 indicates that, as shown in Figure 4, most distances were measured slightly too short with the NavVis VLX systems. Overall, using control points in the adjustment process slightly increases accuracy, with the mean deviation of the spatial distances in both setups being within 6 mm of the manufacturer's specifications.

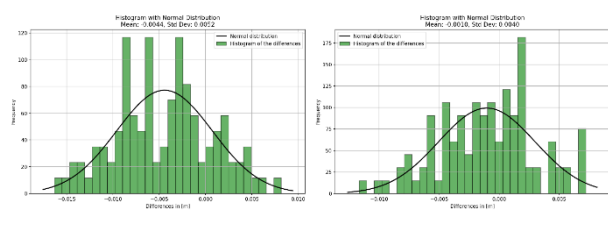


Figure 4. Differences in spatial distances in the 3D test field after adjustment with four control points (VLX 2 left, VLX 3 right).

Systems	VLX 2		VLX 3
Dist. comparison (3D)	without	with CP	with CP
# spatial distances	105	105	105
Max. neg. dev. [mm]	-18,1	-15,1	-11,7
Max. pos. dev. [mm]	9,9	6,0	7,2
Span [mm]	28,0	21,2	18,9
Average value [mm]	-2,5	-3,8	-1,0
Std. dev. av. value [mm]	0,5	0,4	0,0

Table 5. Deviations for the 3D distances of the NavVis VLX 2 after adjustment without and with four control points (CP), while for VLX 3 an adjustment only with four control points was performed.

6.2 Investigations into the influence of incorrect coordinates

The following investigations involved simulating erroneous coordinates of the control points in the VLX 2 dataset adjustments, in order to estimate the influence of erroneous observations. No simulations were calculated for the VLX 3 dataset, as very similar results were expected based on the IVION software. The adjustment was based on four control points (Figure 5, left, green boxes). In the first experiment, an error of +10 cm was simulated in the X coordinate of control point P1. This incorrect input was not detected by the adjustment software, as improvements to the control points are limited to a maximum of 6 mm. It is notable that the error does not appear in control point 1, as the double measurement of this point results in higher weighting of the coordinates in the adjustment. It was only

through independent follow-up measurements of the control points in CloudCompare using control point 1 and 11 as check points that the deviations in the coordinates of all check points close to control point 1 and 11 became visible (Table 6, right), as can be seen in the deviation vectors in Figure 5. This error therefore has a distance-dependent effect on the coordinates of the other points, and consequently on the point cloud.

CP	ΔX	ΔY	ΔZ
	[mm]		
P1_1	2	-1	0
P1_2	3	-1	0
P6	-6	-3	-2
P10_1	0	1	0
P10_2	-2	1	4
P11	3	4	-3

ChP	ΔX	ΔY	ΔZ
	[mm]		
P1	94	-5	9
2	63	-16	7
3	39	-10	-3
4	19	-9	9
7	-7	8	2
8	-2	9	-16
9	15	12	10
P11	55	24	1
12	57	36	2
13	108	28	7
14	115	-5	5
15	107	22	-6
16	84	21	0
17	50	-4	2
18	30	21	3

Table 6. Experiment 1: Deviations at the control points (CP) (left) after adjustment and at the check points (ChP) as well as at two control points (right) after measurements in CloudCompare.



Figure 5. Control points (green boxes) and erroneous point 1 (red) as well as spatial vectors of the coordinate differences in position and height (right, 10x magnification) after adjustment with the erroneous control point 1.

In the second experiment, control point 6 was changed as a polygonal course error in all coordinate directions as follows $X = +4$ cm, $Y = +10$ cm, $Z = -3$ cm. The adjustment resulted in deviations of up to 8 cm at control point 6 (see Table 7, left), indicating an error at this point. This error can therefore be detected and localised at control point 6. In this case, the error is also influenced by the fact that the point has only been measured once by the NavVis VLX 2 system. Deviations of up to 11 mm are visible in the coordinates of three control points (Table 7, right), but these do not allow the error to be clearly assigned, as can be seen from the small error vectors (Figure 6, right).

Several coordinate errors were introduced in the control points of the third experiment: $P1X = +10$ cm, $P6Z = +20$ cm, $P10X = -2$ cm, $P10Y = +2$ cm, $P10Z = +2$ cm and $P11Y = +4.4$ cm. Following adjustment, significant discrepancies were observed at control points 6 and 11 (Table 8 on the left and Figure 7 on the right), whereas no errors were detected at control points 1 and 10. This confirms again that control points with two measurements are given greater weighting in the adjustment process. Measurements of the control points and two control points in CloudCompare also document errors of up to 12 cm in some coordinates. While an error can be detected in this manipulated

dataset, it cannot be localised due to the large number of errors. Therefore, the effects of the manipulation also affect the geometric quality of the point cloud.

CP	ΔX	ΔY	ΔZ
	[mm]		
P1_1	14	-28	0
P1_2	14	-30	1
P6	-37	78	0
P10_1	7	-24	-5
P10_2	6	-22	-2
P11	16	-26	5



Table 7. Experiment 2: Deviations at the control points CP (left) after adjustment and at the check points ChP as well as at two control points (right) after measurements in CloudCompare.

ChP	ΔX	ΔY	ΔZ
	[mm]		
P1	0	-9	-7
2	-2	0	2
3	-1	-3	-5
4	3	3	7
7	-2	1	-4
8	3	6	-8
9	8	-6	-1
P11	-1	-8	6
12	7	11	9
13	1	-8	1
14	0	-11	5
15	1	-3	-5
16	-3	1	1
17	-3	-5	8
18	-3	11	1

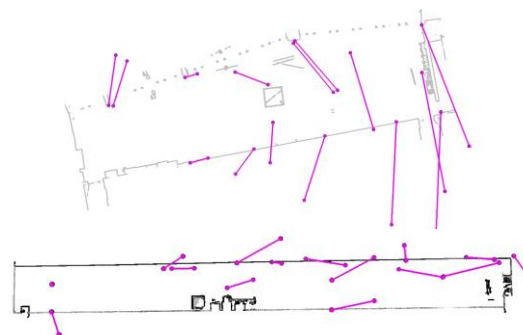


Figure 7. Control points (green boxes) and control points with errors (red, left) as well as spatial vectors of the coordinate differences in position and height (top and bottom right, 10x magnification) after adjustment with control points 1, 6, 10 and 11.

6.3 Sphere spacing error in the mobile 3D test field

In the mobile 3D test field, which has a measuring volume of 2 m × 2 m × 2 m (Figure 8), the sphere spacing error of seven scales, each with spheres at both ends, was determined in accordance with Sheet 2 of VDI/VDE 2634 (2012). Reference measurements were carried out again using the Leica ATR 960 laser tracker and T-Scan. To determine the scale distances, the sphere radii and centres were derived by modelling the spheres appropriately in the point cloud. The mean sphere radius value was determined with deviations of 2.3 mm (VLX 2), -0.9 mm (VLX 3.0) and 0.4 mm (IMAGER 5016). The derived sphere spacing error using the NavVis VLX 2 ranges from 0.5 mm to 1.5 mm, which is therefore systematically slightly too short. In contrast, the sphere spacing error of the VLX 3 is systematically slightly too long, ranging from -0.3 mm to -1.5 mm (Table 9). The same systematic error was derived for the sphere spacing error of the TLS IMAGER 5016; however, the highest value was -3.4 mm due to a sphere that was not completely scanned. The sphere spacing errors of the two NavVis VLX devices were similar to those achieved with the precise terrestrial laser scanner IMAGER 5016.

	Reference [mm]	VLX 2 Δs [mm]	VLX 3 Δs [mm]	IMAGER 5016 Δs [mm]
Sphere radius	72,7	2,3	-0,9	0,4
Scale bar 1	2272,6	1,7	-0,9	-1,5
Scale bar 2	1772,3	0,5	-0,3	-1,6
Scale bar 3	1773,5	1,0	-1,2	-3,4
Scale bar 4	1772,6	0,8	-1,2	-1,2
Scale bar 5	1772,5	0,9	-0,6	-1,1
Scale bar 6	1773,0	0,6	-0,7	-0,6
Scale bar 7	1772,4	1,5	-1,5	-0,2
Mean value		1,0	-0,9	-1,4

Table 9. Sphere spacing error.



Figure 8. Recording of the mobile 3D test field with seven sphere scales to determine the sphere spacing error using VLX 2.

CP	ΔX	ΔY	ΔZ
	[mm]		
P1_1	-1	-1	1
P1_2	0	-1	1
P6	-62	-27	-176
P10_1	4	0	-9
P10_2	1	1	-1
P11	49	476	12



Table 8. Experiment 3: Deviations at the control points CP (left) and at the check points ChP and two control points (right).

ChP	ΔX	ΔY	ΔZ
	[mm]		
P1	98	-3	7
2	61	-18	6
3	25	-17	-6
4	5	-17	0
7	-49	5	0
8	-46	1	-13
9	-3	12	8
P11	47	41	15
12	48	41	4
13	115	45	15
14	122	2	-1
15	111	24	4
16	72	22	13
17	38	-2	2
18	12	31	17

6.4 Comparison of NavVis VLX 2 vs. terrestrial laser scanner Z+F IMAGER 5016

The fourth part of the investigation involved comparing the point clouds from the NavVis VLX 2 and the Z+F IMAGER 5016 terrestrial laser scanner at various locations within the survey area. A total of 66 scans were taken at a resolution of 6.3 mm at a distance of 10 metres. The individual terrestrial laser scanner scans could be registered with each other with a maximum accuracy of 2.6 mm and georeferenced using control points. Based on the higher accuracies provided by the manufacturer's specifications and confirmed by previous laboratory-based geometric investigations (Kersten & Lindstaedt, 2022), it was assumed that the terrestrial laser scanner point cloud could be used as a reference for comparison with the NavVis VLX 2.

The study was carried out using eight vertical sections at 10 m intervals (Figure 9) and two horizontal sections at 3.5 m intervals. As the vertical sections are further away from the control points used in the geodetic laboratory on the third floor, there are greater deviations in position, up to 9 mm, and especially in the height component, up to 17 mm, from the reference (Table 10). This demonstrates that the position and height of the point cloud vary with distance from the control points. The smallest deviations were found in sections 5-7, which are close to the geodetic laboratory on both the third and second floors.

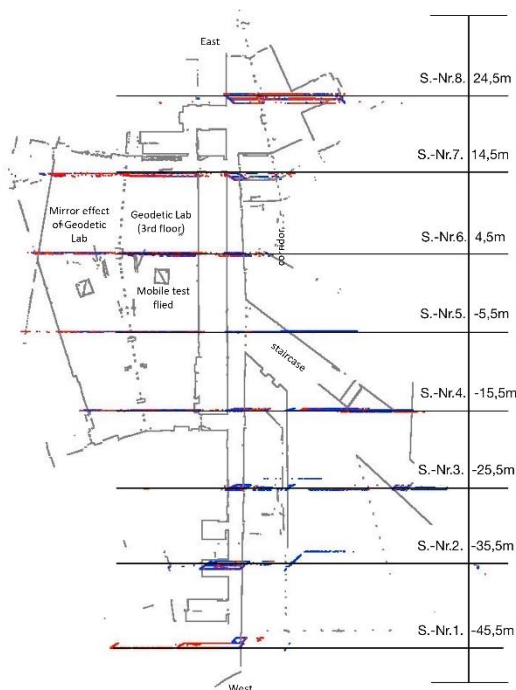


Figure 9. Overview of the vertical sections.

section	deviation 3rd floor [mm]		deviation 2nd floor [mm]	
	Δz	Δxy	Δz	Δxy
1	nan	14	nan	15
2	7	5	-5	17
3	8	4	-4	15
4	8	-3	-4	13
5	7	-3	-5	6
6	-4	-3	-5	4
7	-4	-3	-5	5
8	-9	-5	-5	5

Table 10. Deviations of the NavVis VLX 2 scans to reference.

The NavVis point cloud has minimal occlusion due to the constant movement of the system during recording, which meant that the interiors were captured from different angles. The instrument can also be moved and rotated if an object is obscured, enabling areas that would be inaccessible to a terrestrial laser scanner to be recorded. Despite filtering in the IVION software, there is slight noise on the NavVis point cloud surface (centre right in Figure 10) and wavy effects and rounded edges compared to the laser scanner point cloud (top right and bottom right in Figure 10). Additionally, there is a slight shift of the point cloud relative to the reference at certain locations within the test area, reaching up to 1.7 cm (Figure 10 centre).

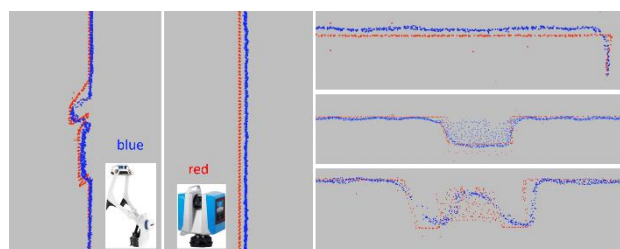


Figure 10. Detail of section 2 on the 3rd floor (left) and 2nd floor (centre), detail of section 3 on the 2nd floor with right-hand side of wall and ceiling (top right), detail of section 6 with motion detector in the corridor of the 3rd floor (centre right) and detail of section 4 showing a motion detector on the 3rd floor (bottom right).

7. Assessment of the results

This chapter evaluates the results based on a detailed analysis of the examined systems. Various criteria are employed to provide a thorough evaluation.

NavVis systems offer a fast and efficient way to capture diverse and complex indoor environments. The lightweight capture device is easy to handle, and the ability to simultaneously capture colour panoramas and 3D point clouds opens up a wide range of applications. Simple operation and control via the AMOLED multi-touch display enables efficient data capture and ensures user-friendliness.

The IVION software's almost fully automated processing of data in the cloud saves users' computing resources. However, some users, especially those working on governmental projects, may doubt the security of data in the cloud. While the small number of parameters to be set and the automatic filtering contribute to the efficiency of the evaluation process, they may also affect the quality of the point clouds, resulting in 'rounded corners' (Figures 10 and 11). However, the cloud-based IVION software is a black box in that the user has no options, such as the ability to switch on other filters.

The results are presented on a comprehensive web platform. Statements about the achieved accuracy are rather limited and essentially restricted to the residuals of the control point coordinates. Following equalisation, products can be output in the form of a filtered point cloud, 360° panoramas and sections.

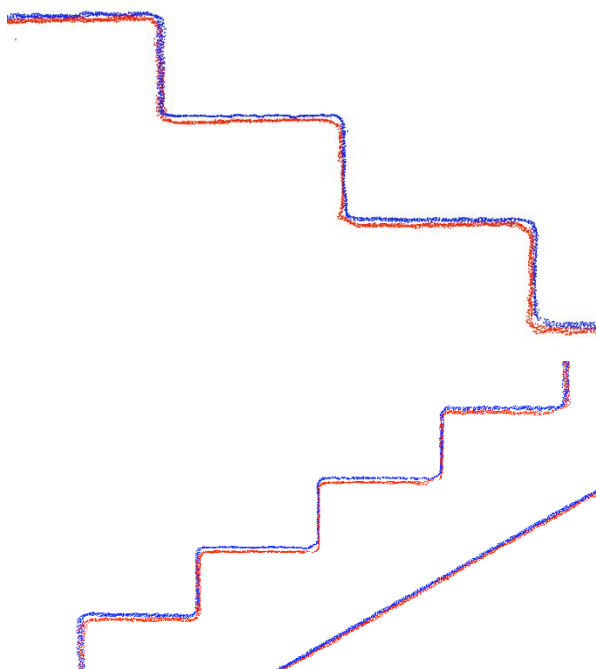


Figure 11. Comparison of point clouds on the steps of the staircase – VLX 2 (red), VLX 3 (blue).

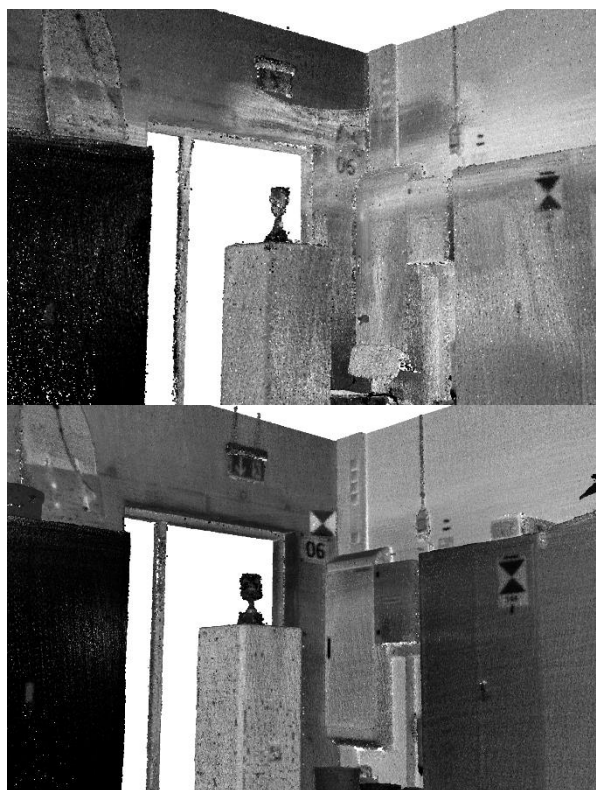


Figure 12. Visualisation of the difference in point density of the VLX 2 (top) and VLX 3 (bottom) in the Geodetic lab, especially at target number 6 (the control point) in the centre of the figure.

The study showed that errors in the control point coordinates are a critical issue, as these errors can only be detected, localised, and eliminated under certain conditions. It is important to give equal weighting to the control points when making adjustments for single or multiple measurements; otherwise, an error in the

coordinates of a higher-weighted point cannot be detected or localised.

The results of the various geometric analyses largely confirmed the manufacturer's technical specifications, achieving an accuracy of 6 mm. However, the accuracy of the NavVis VLX 2 depends on the spatial distribution and distance of the control points. Loop closure is also an important factor in stabilising the adjustment. In the geodetic laboratory area, the 6 mm accuracy could be maintained; however, the corridor sections further away from the control points showed greater deviations in position and height from the reference system. Therefore, a tachymetric survey with a comprehensive design and implementation of well-distributed control points is required to maintain the necessary level of accuracy.

8. Conclusion and outlook

This article presents the results of geometric accuracy tests conducted in the laboratory using the NavVis VLX 2 and VLX 3 recording systems. These systems have proven to be efficient and user-friendly tools for measuring interior spaces. Important features contributing to the user-friendliness of the system include efficient data acquisition, simple handling and versatility in capturing colour panoramas and point clouds. Automated data processing and web-based presentation of results also contribute to the system's overall efficiency.

Geometric analysis of the system shows that using control points significantly improves accuracy and reliability. Tests confirmed that the manufacturer's specified accuracy of 6 mm (1 sigma) was achieved. However, it also became clear that the system's accuracy depends heavily on the distribution and spacing of the control points, as well as the number and distribution of the loop closures.

The NavVis VLX 2 and VLX 3 mobile recording systems produced accurate and complete 3D point clouds when compared to the IMAGER 5016 terrestrial laser scanner. However, the comparison revealed certain inaccuracies in the recording of surface structures and in the spatial position of the point cloud. Deviations between the two NavVis systems and the IMAGER 5016 range from 5 to 13 mm for surfaces and stairs (Figure 11). The point density of the VLX 3 is slightly higher than that of the VLX 2 (Figure 12 for an example). This results in a more complete point cloud at the same recording speed, which in turn significantly increases efficiency. All three systems are in the same price range.

Overall, the NavVis VLX 2 and VLX 3 systems offer high accuracy and flexibility for use in Building Information Modelling (BIM). The coloured point clouds and 360° panoramas provide reliable data for interpreting the materials in the evaluation. These investigations have also shown that using tacheometrically measured control points is essential for reliably meeting the high accuracy requirements of mobile interior space capture.

Acknowledgements

We would like to thank Dipl.-Ing. Thorsten Klaus and Dipl.-Ing. Harald Seeger (both of NavVis GmbH) for kindly providing us with the NavVis VLX 2 recording system and assisting us with the data acquisition. Our thanks also go to Dr Daniel Wujanz (Technet GmbH, Berlin) for his help with analysing the IMAGER 5016 scans and for his valuable input of good ideas into the investigation of the NavVis VLX 2.

References

- Askar, C., Scheider, A., Sternberg, H., 2023: Evaluation of a State-of-the-Art Indoor Mobile Mapping System in a Complex Indoor Environment. *zfv – Zeitschrift für Geodäsie, Geoinformation und Landmanagement*, 148(5), 300-309, <https://doi.org/10.12902/zfv-0445-2023>.
- Business Wire, 2020: Velodyne Lidar Sensors Power 3D Data Capture in New NavVis VLX Mapping System. <https://www.businesswire.com/news/home/20200512005188/en/Velodyne-Lidar-Sensors-Power-3D-Data-Capture-in-New-NavVis-VLX-Mapping-System>, last access on 30.09.2025.
- Campi, M., Falcone, M., Sabbatini, S., 2022: Towards Continuous Monitoring of Architecture. Terrestrial Laser Scanning and Mobile Mapping System for the Diagnostic Phases of the Cultural Heritage. *The International Archives of the Photogrammetry, Remote Sensing and Spatial Information Sciences*, 46, 121-127, <https://doi.org/10.5194/isprs-archives-XLVI-2-W1-2022-121-2022>.
- Digital Twin Consortium, 2022: The Definition of a Digital Twin. <https://www.digitaltwinconsortium.org/hot-topics/the-definition-of-a-digital-twin/>, last access on 30.09.2025.
- Fritsch, D., 2014: Mobile Mapping - Eine Revolution im Vermessungswesen? Schriftenreihe der Stiftung Bauwesen zu „Der Bauingenieur und die Gesellschaft“, Mobilität im Wandel, 18, 39-51, https://www.stiftung-bauwesen.de/wp-content/uploads/2017/09/StiftungBauwesen_2013_Mobilit%C3%A4t-und-Wandel.pdf, last access on 30.09.2025.
- Gebert, F., 2023: Development of an Autonomous Mobile Mapping Robot by Combining the NavVis VLX with the Boston Dynamics SPOT. Master thesis, University of Applied Sciences Munich, <https://opus4.kobv.de/opus4-hm/frontdoor/index/index/docId/450>, last access on 30.09.2025.
- Gharineiat, Z., Tarsha Kurdi, F., Henny, K., Gray, H., Jamieson, A., Reeves, N., 2024. Assessment of NavVis VLX and BLK2GO SLAM Scanner Accuracy for Outdoor and Indoor Surveying Tasks. *Remote Sensing*, 16(17), 3256, <https://doi.org/10.3390/rs16173256>.
- Haaranen, D., 2022: Point Cloud Quality of SLAM based Mobile Laser Scanners. *Photogrammetric Journal of Finland*, 28(1).
- Hesai, 2025: Mid-Range Lidar XT16/32/32M. <https://www.hesaitech.com/product/xt16-32-32m/>, last access on 30.09.2025.
- Kersten, T., Lindstaedt, M., 2022: Geometric accuracy investigations of terrestrial laser scanner systems in the laboratory and in the field. *Applied Geomatics*, 14, 421-434, <https://doi.org/10.1007/s12518-022-00442-2>.
- Lehtola, V. V., Kaartinen, H., Nüchter, A., Kaijaluo, R., Kukko, A., Litkey, P., Honkavaara, E., Rosnell, T., Vaaja, M.T., Virtanen, J.-P., Kurkela, M., El Issaoui, A., Zhu, L., Jaakkola, A., Hyypä, J., 2017: Comparison of the Selected State-of-the-art 3D Indoor Scanning and Point Cloud Generation Methods. *Remote Sensing*, 9(8), 796, <https://doi.org/10.3390/rs9080796>.
- NavVis, 2021: State of Mobile Mapping. https://f.hubspotusercontent40.net/hubfs/3339696/211116_NavVis_Mobile_Mapping_Survey_DE.pdf?hsCtaTracking=9cf02bd-d-438f-4d5a-a848-3e83e9364356%7C93874dd8-d0f7-4cfc-90c8-8600598ff722, last access on 30.09.2025.
- NavVis, 2024a: NavVis VLX 2 – Data sheet. <https://www.navvis.com/resources/specifications/navvis-vlx-2>, last access on 30.09.2025.
- NavVis, 2024b: NavVis VLX 3 – Data sheet. <https://www.navvis.com/resources/specifications/navvis-vlx-3>, last access on 30.09.2025.
- Rosen, R., von Wichert, G., Lo, G., Bettenhausen, K. D., 2015: About the Importance of Autonomy and Digital Twins for the Future of Manufacturing. *Ifac-papersonline*, 48(3), 567-572, <https://doi.org/10.1016/j.ifacol.2015.06.141>.
- Schmidt, J., Volland, V., Iwaszczuk, D., Eichhorn, A., 2023: Detection of Hidden Edges and Corners in Slam-Based Indoor Point Clouds. *The International Archives of the Photogrammetry, Remote Sensing and Spatial Information Sciences*, 48, 443-449, <https://doi.org/10.5194/isprs-archives-XLVIII-1-W1-2023-443-2023>.
- Sekine, R., Tomizawa, T., Tarao, S., 2023: Trial of utilization of an environmental map generated by a high-precision 3D scanner for a mobile robot. *Journal of Robotics and Mechatronics*, 35(6), 1469-1479, <https://doi.org/10.20965/jrm.2023.p1469>.
- Stachniss, C., 2017: Simultaneous Localization and Mapping. In C. Heipke (Hrsg.), *Photogrammetrie und Fernerkundung: Handbuch der Geodäsie*, herausgegeben von Willi Freuden und Reiner Rummel, Springer Berlin Heidelberg, 293-320, https://doi.org/10.1007/978-3-662-46900-2_37-1.
- VDI/VDE 2634, 2012: Optical 3-D measuring systems - Optical systems based on area scanning. VDI/VDE guideline 2634, part 2, Beuth Verlag, Berlin.
- VectorNav Technologies, 2025: VN-100 IMU/AHRS. <https://www.vectornav.com/products/detail/vn-100>, last access on 30.09.2025.